patients surgically treated at one institution during 1940 through 1989. *Surgery* 1993;114:1050–1058.
5. Mazzaferri EL, Jhiang SM. Long-term impact of initial surgical and medical therapy on papillary and follicular thyroid cancer. *Am J Med* 1994;97:418–428.
6. Zimmermann D, Hay ID, Gough IR, et al. Papillary thyroid cancer in children and adults: long-term follow-up of 1039 patients conservatively treated at one institution during three decades. *Surgery* 1988;104:1157–1166.
7. La Quaglia MP, Corbally MT, Heller G, et al. Recurrence and morbidity in differentiated thyroid carcinoma in children. *Surgery* 1988;104:1149–1156.
8. Harness JK, Thompson NW, McLeod MK, et al. Differentiated thyroid carcinoma in children and adolescents. *World J Surg* 1992;16:547–554.
9. Segal K, Sidi J, Levy R, et al. Thyroid carcinoma in children and adolescents. *Ann Otol Rhinol Laryngol* 1985;94:346–349.
10. Tallroth E, Backdahl M, Einhorn J, et al. Thyroid carcinoma in children and adolescents. *Cancer* 1986;58:2329–2332.
11. Schlumberger M, De Vathaire F, Travagli JP, et al. Differentiated thyroid carcinoma in childhood: long term follow-up of 72 patients. *J Clin Endocrinol Metab* 1987;65: 1088–1094.
12. Ceccarelli C, Pacini F, Lippi F, et al. Thyroid cancer in children and adolescents. *Surgery* 1988;104:1143–1148.
13. Descardins JG, Bass J, Leboeuf G, et al. A 20-year experience with thyroid carcinoma in children. *J Pediatr Surg* 1988;23:709–713.
14. Lamberg BA, Karkinen-Jööskelöinen M, Franssila KO. Differentiated follicle-derived thyroid carcinoma in children. *Acta Paediatr Scand* 1989;78:419–425.
15. McWhirter WR, Stiller CA, Lennox EL. Carcinomas in childhood: a registry-based study of incidence and survival. *Cancer* 1989;63:2242–2246.
16. Merrick Y, Hansen HS. Thyroid cancer in children and adolescents in Denmark. *Eur J Surg Oncol* 1989;15:49–53.
17. Samuel AM, Sharma SM. Differentiated thyroid carcinomas in children and adolescents. *Cancer* 1991;67:2186–2190.
18. Thoresen S, Akslen LA, Glattre E, et al. Thyroid cancer in children in Norway 1953–1987. *Eur J Cancer* 1993:29A:365–366.
19. Vassilopoulou-Sellin R, Klein MJ, Smith TH, et al. Pulmonary metastases in children and young adults with differentiated thyroid cancers. *Cancer* 1993;71:1348–1352.
20. Jocham A, Joppich I, Hecker W, et al. Thyroid carcinoma in childhood: management and follow up of 11 cases. *Eur J Pediatr* 1994;153:17–22.
21. Stael APM, Plukker JM, Piers DA, et al. Total thyroidectomy in the treatment of thyroid carcinoma in childhood. *Br J Surg* 1995;82:1083–1085.
22. World Health Organization. International histological classification of tumours. In: *Histological typing of thyroid tumours; Geneva: World Health Organization, 1969–1981*, 2nd ed. Berlin: Springer-Verlag 1988:11–12.
23. Hermanek P, Sobin LH, eds. *UICC TNM classification of malignant tumours*, 4th ed. Berlin: Springer-Verlag 1987.
24. Mazzaferri EL. Treating high thyroglobulin with radioiodine: a magic bullet or a shot in the dark? [Editorial] *J Clin Endocrinol Metab* 1995;80:1485–1487.
25. Pacini F, Lippi F, Formica N, et al. Therapeutic doses of I131 reveal undiagnosed metastases in thyroid cancer patients with detectable serum thyroglobulin levels. *J Nucl Med* 1987;28:1888–1891.
26. Scheumann GFW, Gimm O, Wegener G, et al. Prognostic significance and surgical management of locoregional lymph node metastases in papillary thyroid cancer. *World J Surg* 1994;18:559–568.
27. Sessions RB, Davidson JB. Thyroid cancer. *Med Clin North Am* 1993;77:517–538.
28. van den Brekel MWM, Casteljins JA, Snow GB. Detection of lymph node metastases in the neck: radiologic criteria. *Radiology* 1994;192:617–618.
29. Frankenthaler RA, Sellin RV, Cangir A, et al. Lymph node metastasis from papillary-follicular thyroid carcinoma in young patients. *Am J Surg* 1990;160:341–343.
30. Dottorini ME, Lomuscio G, Mazzucchelli L, et al. Assessment of female fertility and carcinogenesis after Iodine-131 therapy for differentiated thyroid carcinoma. *J Nucl Med* 1995;36:21–27.
31. Pacini F, Gasperi M, Fugazzola L, et al. Testicular function in patients with differentiated thyroid carcinoma treated with radioiodine. *J Nucl Med* 1994;35:1418–1423.
32. Williams D. Thyroid cancer and the Chernobyl accident. *J Clin Endocrinol Metab* 1996;81:6–8.
33. Risica S. The environmental risk in power production: experimental results, calculations and considerations after Chernobyl. *Ann Ist Super Sanita* 1987;23:177–522.
34. Nikiforov Y, Gnepp DR. Pediatric thyroid cancer after the Chernobyl disaster: pathomorphologic study of 84 cases (1991–1992) from the Republic of Belarus. *Cancer* 1994:74:748–766.
35. Nikiforov Y, Gnepp DR, Fagin JA. Thyroid lesions in children and adolescents after the Chernobyl disaster: implications for the study of radiation tumorigenesis. *J Clin Endocrinol Metab* 1996;81:9–14.

Imaging Prostate Cancer with Technetium-99m-7E11-C5.3 (CYT-351)

Vaseem U. Chengazi, Mark R. Feneley, David Ellison, Maria Stalteri, Arthur Granowski, Marie Granowska, Cyril C. Nimmon, Stephen J. Mather, Roger S. Kirby and Keith E. Britton

Departments of Nuclear Medicine and Urology, and Imperial Cancer Research Fund Nuclear Medicine Group, St. Bartholomew's Hospital, London, United Kingdom

To evaluate the performance of the ^{99m}Tc-labeled monoclonal antibody CYT-351 in visualizing prostate cancer, radioimmunoscintigraphy (RIS) was performed in 35 patients. **Methods:** Antibody (0.5 mg) labeled with 600 MBq ^{99m}Tc was injected intravenously after obtaining informed consent. Planar and SPECT imaging was performed at 10 min and 6–8 and 22–24 hr postinjection. The scans were evaluated for visualization of the primary focus or local recurrence, extraprostatic invasion, lymph node involvement and uptake in bone and soft tissue metastases. **Results:** Thirty-six studies in 35 patients were performed. In 13/14 evaluable studies with clinically localized prostate cancer, RIS had a true-positive rate of 92% (12/13). In eight patients with previous incidental carcinoma detected during transurethral resection undertaken for clinically benign disease, there were 86% true-positive results (6/7) and one true-negative result, which were confirmed by systematic needle biopsies. In six patients with evidence of local recurrence after a previous radical prostatectomy, the true-positive rate was 100% (6/6), which was confirmed by raised or rising prostate-specific antigen levels (PSA) and/or by biopsy. In the eight patients with known metastases, the disease was visualized in 4/4 with progression but not in the 3/3 with regression; one patient demonstrated regressing disease as determined by PSA levels. The overall accuracy was 92%. **Conclusion:** RIS with ^{99m}Tc CYT-351 is capable of providing good quality images and yielding clinically useful information safely. It has a potentially important clinical role for patients with rising PSA levels but negative images by conventional modalities.

Key Words: prostate cancer; technetium-99m; monoclonal antibody; prostate-specific antigen

J Nucl Med 1997; 38:675–682

Prostate cancer, one of the commonest malignancies in men, has large social consequences. The direct medical expenses and those of lost productivity and wages due to morbid complications from local extension and metastatic spread, or from the side effects of treatment, are estimated at four billion dollars annually in the U.S. (*1*). The death rate from prostate cancer increases rapidly with age, and since the population is aging steadily and mortality from other causes is decreasing, the number of deaths from prostate cancer is likely to continue to increase. With further development of current trends to use

Received Jul. 2, 1996; revision accepted Sep. 19, 1996.

For correspondence or reprints contact: Vaseem U. Chengazi, MD, Department of Nuclear Medicine, St. Bartholomew's Hospital, West Smithfield, London EC1A 7BE, United Kingdom.

resources effectively in a managed health care system, the economic burden of prostate cancer is under closer scrutiny.

Much of the suffering and expense due to this disease is related to metastatic spread, which occurs by both lymphatic and hematogenous routes. The first areas of lymphatic metastasis include the obturator and internal and external iliac nodes. Patients with a single microscopic focus of cancer in a lymph node have patterns of progression and cancer-specific death rates that are similar to those of patients with more extensive nodal disease and much worse than those of patients with no nodal metastases. Similarly, the risk of dying of prostate cancer within 10 yr is nearly three times higher (around 60%) for patients with at least one malignant lymph node than for those with no lymph node metastases (*2*).

Early detection of the spread is important for treatment. It is believed that when prostate cancer has spread to the pelvic lymph nodes, the patient has systemic disease (*3*) and can therefore be regarded as a candidate for palliative rather than curative therapy. Correct staging is therefore critical to select the appropriate patients for primary therapy. While staging pelvic lymphadenectomy remains the standard for assessing the status of the pelvic lymph nodes, noninvasive modalities, including ultrasound (US), CT and MRI, are routinely used to evaluate these sites. However, the performance of these modalities that demonstrate primarily the structural manifestations remains less than ideal (*4–7*). Even staging pelvic lymphadenectomy is a sampling procedure and can miss metastatic spread.

Attempts to image prostate cancer using functional characteristics of the tumor by nuclear medicine techniques were first made with zinc radioisotopes, but were limited by lack of sensitivity and specificity (*8*). Subsequently, the use of radiolabeled anti-androgens, estrogens and androgens to target prostatic tissue also failed due to high urinary excretion of the radiolabel and poor specific uptake (*9*). Somewhat more encouraging results were reported using antibodies directed against prostatic-specific antigen (PSA) and prostatic acid phosphatase, but clinical efficacy was still low because of binding of the antibody to the circulating antigen (*10*). Recently, a murine IgG1 monoclonal antibody designated 7E11-C5.3 has been raised against a newly identified membrane antigen present in normal and malignant prostatic tissues (*11*). This antigen is a membrane-bound glycoprotein with a molecular weight of 100,000 and is expressed almost only by prostatic tissue (*12*). Prostatic radioimmunoscintigraphy using the ^{111}In-labeled complex of this antibody, ^{111}In-GYK-DTPA-7E11-C5.3, designated CYT-356, is currently undergoing clinical trials and has shown promise (*13*).

The use of a ^{99m}Tc label for this antibody would offer advantages of reduced imaging time, lower radiation dose and lower cost. This study presents results from ^{99m}Tc-CYT-351 imaging of primary and secondary malignancy and tumor staging in 35 patients with prostatic carcinoma.

MATERIALS AND METHODS

This project was approved by the local City and Hackney District Ethics Committee and the Administration of Radioactive Substances Advisory Committee of the Department of Health and Social Security. The entire procedure was explained to the patient and his informed consent obtained. Attention was paid to any history of allergies, especially for foreign proteins. A positive history would have excluded the patient from the study but none such presented themselves.

Four categories of patients were referred by the urology department: patients before primary prostatectomy, patients with incidental carcinoma (InCaP) found during transurethral resection (TURP) undertaken for clinically benign disease, patients with evidence of local recurrence and patients with evidence of metastases.

Labeling

For the first 31 patients, the antibody was labeled by a modified Schwarz technique as developed by Mather and Ellison (*14*). For the next four patients, a site-specific conjugation method using a hydrazide-linked chelator as described by Stalteri et al. (*15*) was used.

Procedure

After taking a preinjection blood sample and recording the vital signs, 600 MBq of activity attached to 0.5 mg of the antibody was injected intravenously. The vital signs were recorded postinjection as well. Both planar and tomographic studies were performed using a LFOV gamma camera fitted with a general purpose collimator and set with a 15% window around 140 keV. The imaging protocol involved a sequence of images designed to assess serial changes in uptake based on the premise that specific antibody uptake increases with time, whereas nonspecific uptake decreases with time. The series of planar images consisted of anterior and posterior views of the pelvis and chest with 800K counts each and squat views of 400K each at 10 min, 6–8 hr and 22–24 hr postinjection. Pelvic SPECT was done at 6–8 hr and 22–24 hr postinjection, with 64 steps over 360°, each step acquired for 60 sec. To facilitate alignment, additional 30-sec marker views were acquired for anterior pelvis and squat projections, the markers being placed on prominent bony landmarks. The chest views were aligned with help of the liver and splenic borders. Blood samples at preinjection and follow-up were obtained for assessing any human anti-murine antibody (HAMA) response.

Investigations

PSA levels were assessed by the microtiter plate method. HAMA titers were assayed by the Enzygnost microassay kit (Behring, Bremen, Germany). CT was performed on a HiSpeed Advantage and the MR scans on a Signa 1.5T machine. Transrectal ultrasonography was done using an XP-128 (Acuson, Mountain View, CA).

Data Analysis and Interpretation

Image display and analysis was undertaken on a Hermes workstation (Nuclear Diagnostics, Stockholm, Sweden). The SPECT data were reconstructed using a pixel size and thickness of 6.2 mm, a Weiner prefilter customized for the particular collimator and a ramp reconstruction filter. The cutoff frequency was adjusted to the counts by selecting a filter order between 1–33 according to the manufacturer's software instructions. The cutoff was adjusted to the maximum counts according to the following relationship:

$$\text{Filter order} = 5.56^{10}\log\left[\text{Counts}_{max} - (\text{Counts}_{max})^{1/2}\right].$$

Detailed image matching was performed so that a section at 6 hr could be shown to be corresponding to the same section at 24 hr. Studies were interpreted by two experienced blinded observers. Specific uptake increasing with time was interpreted to be due to malignancy, as opposed to nonspecific uptake decreasing with time after an initial distribution in normal structures such as blood vessels. Patterns of specific uptake were interpreted to be due to localized disease if the uptake was confined to the gland, as extraprostatic spread if there was uptake in the periprostatic region with blurring of the margins, involvement of lymph nodes if there was focal uptake in the pelvis and focal uptake in bone and abnormal soft-tissue uptake as metastases. According to these criteria, while diffuse periprostatic uptake may or may not include lymph node involvement as part of extraprostatic spread, the study was reported as being positive for nodal involvement only if a focal pattern of uptake also was seen.

TABLE 1
Clinically Localized Prostate Cancer

Patient	PSA	Ix	BS	L	EP	N	B	Margins
BAI	Raised	T2, CT−, MRI−	−	+	+	−	−	Posterior
GOR	Normal	T1, CT−	−	na	na	na	na	Left
THA	Raised	T2, CT−	−	+	+	−	−	Right, apical posterior,
COP	Normal	T2, CT−	−	+	+	−	−	basal, apical, left seminal vesicle
TED	Raised	T2, CT−	−	+	−	−	−	All margins clear
WHI	Raised	T1, CT: irregular indentation of bladder base	−	+	+	+	−	na
FOR	Raised	T2, CT: na	−	+	+	−	−	Left, apex, base
CAW*	Raised	BPH, CT: na	−	+	−	−	−	Inferior margin
POU†	Raised	CT: loss of periprostatic tissue planes; MRI: ?left neurovascular bundle invasion	−	+	−	−	−	Right lateral, bladder neck, apex, extension into both seminal vesicles
SMI	Raised	CT−, MRI: 1 cm nodule in apex	−	+	+	−	−	Apical
RUB*	Raised	BPH, CT: na	−	+	+	−	−	Inferior margin on left side
COR‡	Raised	T2, CT−, MRI	−	+	−	−	−	Left seminal vesicle, apical margin
HOLW	Normal	BPH, CT−	−	−	−	−	−	na
BRO	Raised	CT−, MRI−	−	+	±	−	−	All margins clear

*Twenty-four-hour SPECT images not available.
†Significant bladder activity in early SPECT images.
‡Asymmetry on left side of bladder on retrospection.
PSA = prostate-specific antigen; Ix = investigations; BS = bone scan; L = local prostatic uptake on RIS; EP = extraprostatic spread on RIS; N = nodal involvement on RIS; B = bony uptake on RIS; T1, T2 = tumor as determined by digital rectal examination; BPH = benign prostatic hyperplasia; + = positive; − = negative; ± = equivocal; na = not applicable.

RESULTS

Thirty-five patients underwent 36 RIS studies, 1 patient having 2 studies 6 mo apart. Fourteen patients had clinically localized prostate cancer diagnosed by US-guided biopsy, eight had previous InCaP identified at TURP undertaken for clinically benign prostatic disease, six had evidence of local recurrence after a previous radical prostatectomy and eight had metastatic disease.

The tumors in this series were mostly adenocarcinomas Gleason grades 2+2 to 3+4 and no correlation was noted between the degree of differentiation and the intensity of specific uptake in any of the groups.

The results of 14 studies in patients with clinically localized disease are given in Table 1. RIS was correctly positive in 12/13 (92%) and one imaging sequence, which could not be completed due to a change in the time of surgery at short notice, was deemed not to be evaluable. Twenty-four-hour SPECT could not be performed in two studies, and the studies were reported on the early SPECT and planar images. The primary focus was seen in 12 studies, whereas seven had clear evidence of extraprostatic spread on RIS. One also had increased uptake in pelvic lymph nodes and CT suggested extraprostatic invasion of the bladder base. In one patient, no specific uptake was visualized. Only one of his five biopsy samples contained neoplastic cells and he had a normal PSA level. Eleven patients subsequently underwent radical prostatectomy and two of these

TABLE 2
Incidental CaP During Transurethral Resection

Patient	PSA	Ix	BS	L	EP	N	B	Rx
BUR	Raised	T1	−	+, Bx+	+	−	−	No
PES	Undetectable	T1	−	−, Bx−	−	−	−	No
BAY	Falling	T1	−	−, Bx+	−	−	−	Hormone
DOL*	Raised	T1	−	+, Bx+	±	−	−	No
RUN1	Rising	T1	−	+, Bx+	+	−	−	PreRP
SER	Rising	T1	−	+, Bx+	+	−	−	PostRT
MOO	Raised	T1	−	±, Bx+	−	−	−	PreRP
HUS†	Normal	T1, CT−, MRI: ?Invasion of capsule posteriorly		+, Bx+	−	−	−	No

*Large hot bladder.
†No 24-hr SPECT images.
InCaP = incidental carcinoma; TURP = transurethral resection; PSA = prostate specific antigen; Ix = investigations; BS = bone scan; L = local prostatic uptake on RIS; EP = extraprostatic spread on RIS; N = nodal involvement on RIS; B = bony uptake on RIS; Rx = treatment; Bx = biopsy; PreRP = preradical prostatectomy; PreRT = preradical radiotherapy; T1 = tumor as determined by digital rectal examination; + = positive, − = negative; ± = equivocal.

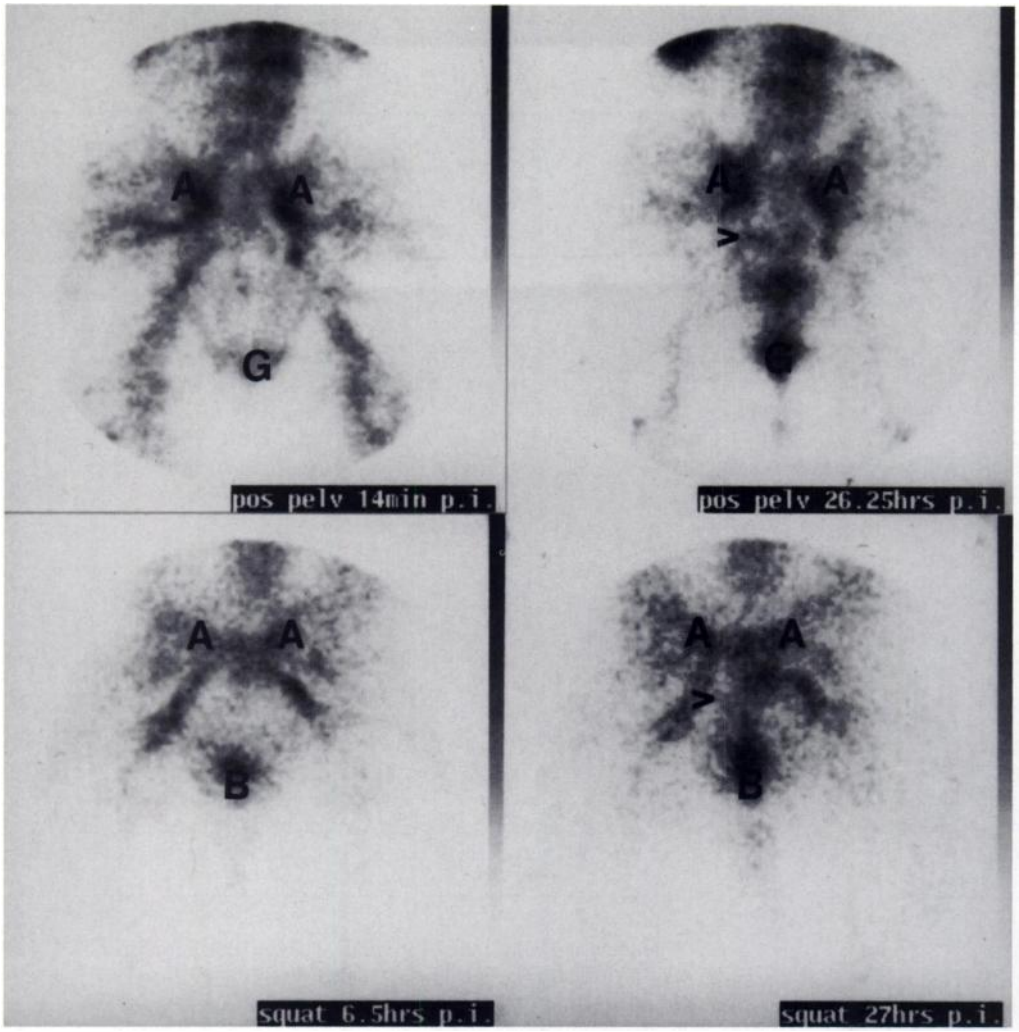

FIGURE 1. Prostate cancer: ^{99m}Tc-CYT-351 planar imaging. (Top left) Posterior view of the pelvis at 14 min postinjection (p.i.). (Top right) Posterior view of the pelvis at 26 hr p.i. (Bottom left) Squat view of the pelvis at 6 hr p.i. (Bottom right) Squat view of the pelvis at 27 hr p.i. Uptake is seen superior to the bladder on the posterior view at 26 hr but not at 14 min, and posterior to the bladder on the squat view at 27 hr but not at 6 hr, indicating specific time-dependent uptake of the antibody by the extraprostatic spread of the cancer. A = sacroiliac joints; B = bladder; g = genitalia; arrowheads = abnormal uptake.

patients had complete excision with negative surgical margins. RIS was correctly negative for extraprostatic spread in one and was judged to be equivocal in the other. One patient subsequently showed rapid disease progression with rising PSA levels, but the bone scan was still negative 6 mo later. Histological examination of his radical prostatectomy specimen had confirmed vascular, perineural and surgical margin invasion and a subsequent US guided biopsy confirmed local soft-tissue recurrence.

The results of eight studies in patients with InCaP identified during TURP are given in Table 2. RIS was correctly positive in 6/7 (86%) and correctly negative in one. Four patients were untreated and four were being treated, one with hormone manipulation, one with radical radiotherapy and two with biopsy-proven residual disease underwent radical prostatectomy. Twenty-four-hour SPECT could not be performed in one study and was reported without these images. One of the patients, initially referred with a diagnosis of prostate cancer but who was not undergoing treatment, had negative RIS and negative repeat biopsies. His PSA levels remained undetectable. The other three not on treatment had biopsy-proven evidence of disease, which was visualized on RIS and correlated with PSA levels in two patients. One had a normal PSA level in spite of a positive biopsy. These three patients are undergoing additional follow-up. The patient treated with hormones had a negative RIS but a positive biopsy. His PSA had fallen from 128 ng/ml to undetectable levels at the time of RIS. The patient who had previously been treated with radical radiotherapy had PSA evidence of further disease progression. Figure 1 shows the time dependency of the specific uptake in this patient's positive RIS, which was confirmed by biopsy. Of the two patients undergoing radical prostatectomy, one was rescanned 6 mo later and had rising PSA levels. His repeated RIS showed recurrence, which was confirmed by repeated biopsy. Figure 2 shows his early and late RIS images just before radical prostatectomy, whereas Figure 3 shows the same sections 6 mo later. RIS for the other patient was equivocal for the primary focus. His original biopsy was positive in one of three samples. The histology report of the radical prostatectomy specimen showed a well-differentiated tumor extending "very close" to the anterior and "close" to the right lateral margin of resection, but no evidence of extraprostatic spread. He is undergoing follow-up.

Six patients had RIS after radical prostatectomy and their results are given in Table 3. RIS was correctly positive in all, correlating with rising PSA levels and/or biopsy in five, and a high but falling PSA in one. None of these patients had received any adjuvant treatment. Three of these patients had detectable PSA levels ranging between 2.9 and 5.1 ng/ml at least 3 mo after surgery. One had undetectable PSA and was clinically disease-free, although tumor was present at two surgical excision margins. In all patients, RIS demonstrated increased uptake in the prostatic bed compatible with recurrence of the disease. Residual local malignancy was confirmed by US-guided biopsy in two patients. One patient went on to develop bone metastases. The other two patients demonstrated disease progression as shown by rising PSA levels and are undergoing further observation.

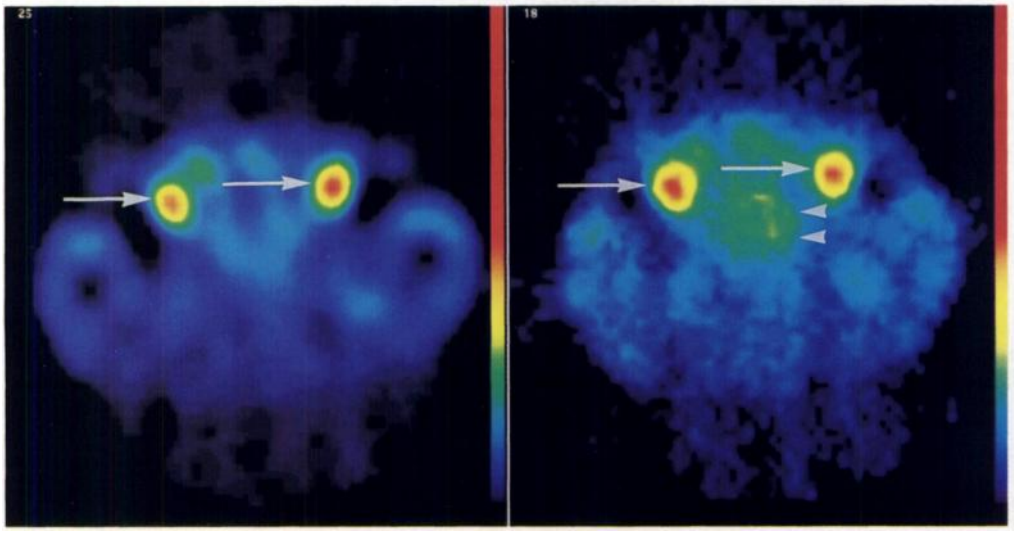

FIGURE 2. Prostate cancer: ^{99m}Tc-CYT-351 SPECT image. Transverse section at 6 hr (left) and the equivalent section at 24 hr (right) show an increase in specific uptake in the prostate indicating malignancy. Arrows indicate external iliac vessels; arrowheads indicate abnormal uptake.

The results of eight men who had known metastatic prostate cancer, seven with bone metastases and one with extensive soft-tissue disease and nodal disease demonstrated by CT, are given in Table 4. RIS correctly visualized the disease in 4/4 patients with progression and not in the 3/4 patients steadily responding to hormone therapy. RIS demonstrated clearly increased uptake of the antibody in the bony lesions in two patients (shown in Fig. 4) and was equivocal in one. The remaining four patients who did not show uptake in bony lesions were all responding to hormone manipulation with falling PSA levels. Soft-tissue disease in the pelvis was seen in five, the negative RIS being in three patients steadily responding to hormone therapy. The overall summary is presented in Table 5.

With the exception of one patient who complained of a minor burning sensation at the injection site, no side effects were experienced. The vital signs remained stable pre- and postinjection in all patients. No significant HAMA responses were detected in any of the patients, all measurements being below 15 μg/ml, the positive cutoff level for the kit being used. No abnormal reaction was noted in the patient having two studies, and the images did not show any increased localization in the liver.

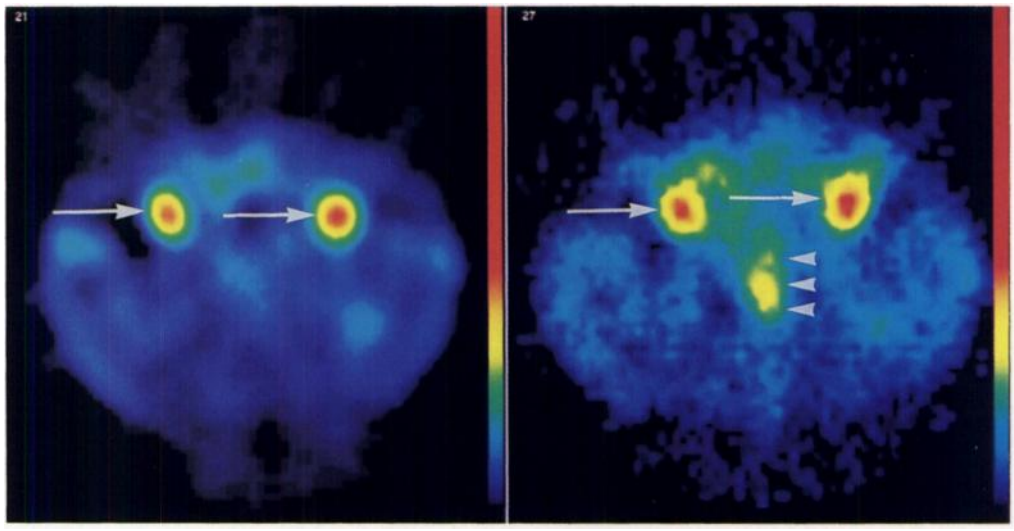

FIGURE 3. Prostate cancer: ^{99m}Tc-CYT-351 SPECT image. Repeat study of patient shown in Figure 2, 6 mo after radical prostatectomy. Image on the left at 6 hr shows an empty prostatic bed and image on the right at 24 hr shows increased specific uptake in the equivalent section. This indicates recurrence of the prostate cancer. Arrows indicate external iliac vessels; arrowheads indicate abnormal uptake.

TABLE 3
Postradical Prostatectomy

Patient	PSA	Ix	BS	Rec	N	B	Rx
YOU	Undetectable	Follow-up	−	+, Bx+	−	−	No
DAV	Rising	Ct−, MRI−	−	+	−	−	Follow-up
RUN2	Rising	TRUS−	+	+, Bx+	−	−	No
LEE	Falling	Follow-up	+, regression	+	−	−	No
SHA	Rising	TRUS−	−	+	−	−	No
SCO	Rising	CT−, MRI−	−	+	−	−	na

PSA = prostate specific antigen; Ix = investigations; BS = bone scan; Rec = recurrence in prostatic bed on RIS; N = nodal involvement on RIS; B = bony uptake on RIS; Rx = treatment; TRUS = transrectal ultrasonography; Bx = biopsy, + = positive; − = negative; na = not applicable.

TABLE 4
Metastatic Disease

Patient	PSA	CT	BS	L	EP	N	B	Rx
NER	Rising	+	−	+	+	+	−	Follow-up
TOL	Falling	na	+, regression	+	±	−	−	Hormone
HAL	Falling	na	+, regression	−	−	−	−	Hormone
PRA	Falling	na	+, regression	−	−	−	−	Hormone
ERL	Falling	−	+	−	−	−	−	Hormone
WAL	Falling	T2	+	+	+	−	+	PostRT
HOLJ	Rising	na	+, widespread metastases	+	+	+	+	Hormone
CHA	Rising	Bilateral nodes R > L	+, widespread metastases	+	+	+	±	Hormone

PSA = prostate specific antigen; BS = bone scan; L = local prostatic uptake on RIS; EP = extraprostatic spread on RIS; N = nodal involvement on RIS; B = bony uptake on RIS; Rx = treatment; PostRT = postradical radiotherapy; T2 = tumor as determined by digital rectal examination; + = positive; − = negative, ± = equivocal; na = not applicable.

DISCUSSION

Decisions regarding the management of patients with prostate cancer depend on knowing the stage of the disease with regard to the local lymph nodes and whether or not metastatic disease is present. Prostatic RIS aims to provide a means of imaging prostatic malignancy based on "tissue characterization," a unique nuclear medicine advantage. This study explores the use of the radioimmunoconjugate ^{99m}Tc 7E11-C5.3, designated CYT-351, in potentially providing a sensitive and specific method of staging prostatic malignancy, imaging the primary tumor, detecting extraprostatic spread and demonstrating lymphatic and other metastases.

Next to the selection of an appropriate antibody, the choice of the radiolabel is important, depending on the kinetics of the chosen antibody. A long half-life radiolabel such as ^{111}In is more appropriate for slow specific uptake, whereas a short half-life radiolabel, such as ^{99m}Tc, can be used if there is sufficient specific uptake of the antibody within a few half-lives to yield a good signal. Related to this are the considerations of gamma-ray energy of the radiolabel, dose injected, counting

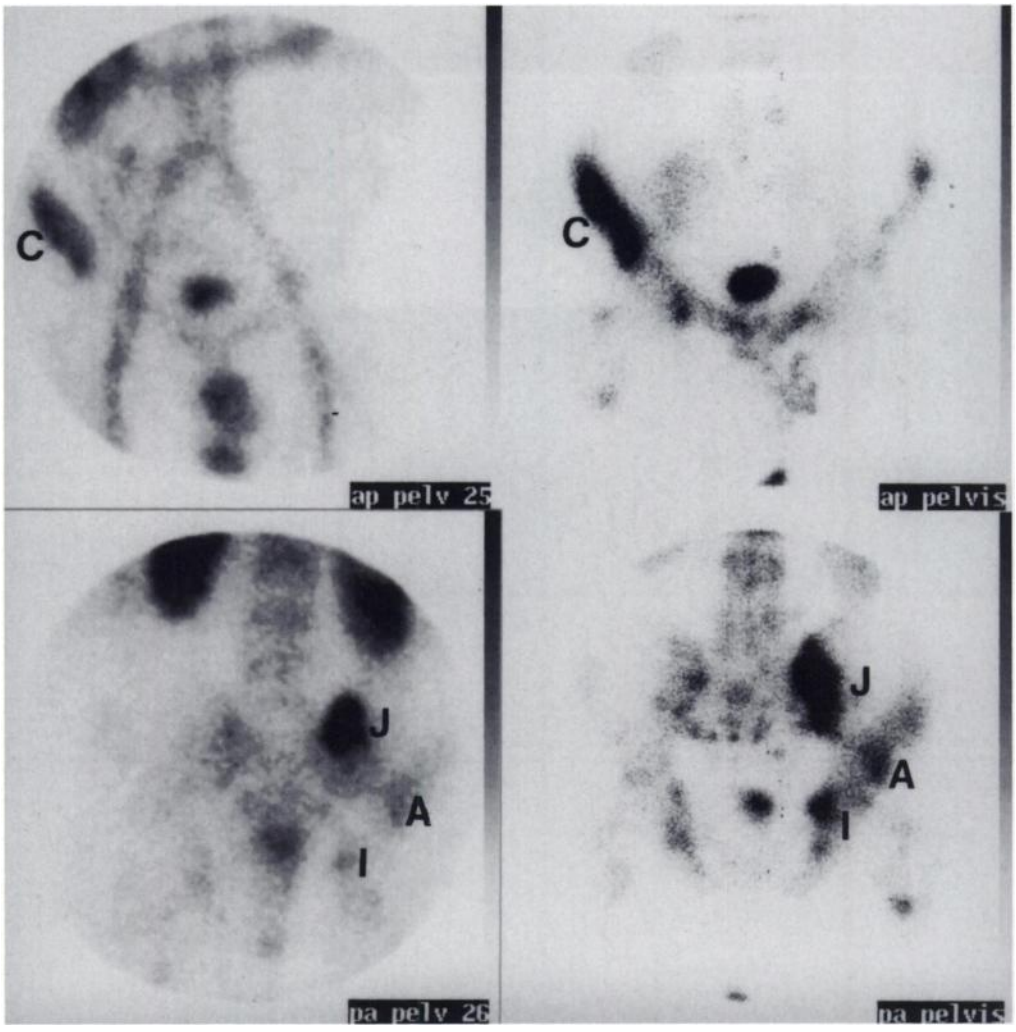

FIGURE 4. Prostate cancer: ^{99m}Tc CYT-351 planar imaging top and bottom left, ^{99m}Tc-MDP bone scan top and bottom right. The 25-hr anterior view of the pelvis (top left) shows specific uptake in the right iliac crest and anterior border, and the posterior view (bottom left) shows specific uptake in the right sacro-iliac region, acetabulum and ischium, all not present at 10 min. The ^{99m}Tc-MDP bone scan at 3 hr p.i. shows corresponding lesions in the anterior (top right) and posterior views (bottom right) of the pelvis. A = acetabulum; C = iliac crest and anterior border; I = ischium; J = sacroiliac joint.

TABLE 5
Summary of Therapeutic Response

Category	RIS positive	Total	Percentage
Clinically localized cancer confirmed by US-guided biopsy	12	13	92 TP
Previous InCaP at TURP			
Cancer present at re-operation	6	7	86 TP
Cancer not present at re-operation	1	1	TN
Follow-up imaging			
Raised or rising PSA	4	4	TP
Rising PSA, biopsy positive	1	1	TP
Biopsy positive, undetectable PSA	1	1	TP
Known metastatic disease			
Rising or high PSA	4	4	TP
Treated and with falling PSA	3	4	75 TN
Total	34	35	92 AC

InCaP = incidental carcinoma; TURP = transurethral resection; PSA = prostate-specific antigen; TP = true-positive; TN = true-negative; AC = accuracy.

rate obtained, signal-to-noise and tumor-to-normal ratios and radiation dose. Apart from the density of antigen expression, the rate of specific uptake depends in a large part on the delivery of the antibody to the tumor by the richness (or paucity) of its vasculature. It has been shown with some success that a high counting rate from a short-lived radiolabel coupled with an appropriate imaging sequence is preferable for imaging (*16,17*).

The initial promise of ^{111}In-GYK-DTPA-7E11-C5.3, designated CYT-356, is now being established further by several groups (*18,19*) in the U.S., and a product license application has been filed with the Food and Drug Administration (*20*).

Due to the characteristics afforded by the use of ^{111}In, a prolonged imaging sequence is adopted, with planar and/or SPECT at intervals up to 3 or 5 days postinjection. There is also considerable marrow uptake, which can be an important consideration within the bony confines of the pelvis and along the vertebral column. This delayed imaging provides sufficient time for the gut excreted portion of the antibody to travel down into the pelvic area, thereby adding another potential distraction, and may require the use of laxatives for elimination.

The use of ^{99m}Tc as presented here has advantages over ^{111}In by virtue of its near ideal physical characteristics, low radiation dose, low cost, easy availability, minimal marrow uptake and a short imaging sequence not requiring laxatives.

However, common to both these radiolabels is the problem of urinary excretion and the resulting "hot" bladder adjacent to the prostate. Moreover, the bladder accumulates activity during SPECT data acquisition. These two factors can cause significant artefacts, which may hinder evaluation.

In this series, one patient had a large hot bladder sufficient to cause significant artefacts, whereas one study had this problem in only the early SPECT imaging at 6 hr. However, the primary focus of disease was visualized in both cases. Catheterization was not included in the protocol because of its low acceptability as an outpatient procedure, and because even this may not be enough to remove the activity in the bladder in these patients. However, the problem of a large range of contrast values in objects that demonstrate considerable change in activity over the period of acquisition of SPECT data is a wider issue that needs to be addressed rigorously at a basic level, especially in studies with monoclonal antibodies where the abnormal-to-normal tissue ratios are not as great as those routinely achieved with other radiopharmaceuticals. Methods for correcting for artefacts caused by a rapidly filling bladder have been studied but the solutions, although leading to significant improvements, are not as yet accurate (*21*). Some preliminary work in dealing with this problem in a more general manner has been undertaken in this department with promising results but further development is required (*22*).

An aspect of the protocol that was felt to be an important aid to interpretation was the comparison between early and late images, not only for the planar images but also particularly the SPECT slices. A customized program was developed in the department to produce matching sections from the 6- and 24-hr SPECT acquisitions in order to assess changes in specific and nonspecific uptake of the antibody. In one study, this was not possible because the imaging sequence had to be abandoned due to a change in the time of surgery at short notice. This study was not evaluated. Two further studies had to be reported without the benefit of the 24-hr SPECT images, and this was felt to reduce the confidence level. However, the primary focus was visualized in both, with evidence of extraprostatic spread in one. The inferior margin on the left side of the surgical margin was invaded by tumor in this patient.

Three patients showed evidence of nodal involvement on RIS. Two of these had extensive pelvic lymphadenopathy demonstrated on CT scanning, which corresponded to areas of increased uptake. The other patient with clinically localized disease had no evidence of lymphadenopathy on CT scanning (but indentation of the bladder base) and has declined treatment in spite of PSA progression from 16–24 ng/ml over 6 mo. These data indicate that nodal metastatic disease may be detected by RIS and its presence is of both prognostic and therapeutic importance. Furthermore, assessment of soft tissue disease other than nodal involvement may be important in management and prognosis, and RIS is well suited to this role. The results in the clinically localized group support this.

Lesions shown by bone scanning may not be shown by RIS after their response to treatment. Bone scans demonstrating osteoblastic activity are not specific for metastatic disease and other conditions causing increased uptake commonly coexist in the elderly, particularly degenerative changes and Paget's disease. Similarly, increased uptake associated with sites previously involved with metastatic disease may persist as abnormalities on a bone scan despite successful treatment. These results suggest that RIS detects only recent and active prostatic bone metastases, i.e., a subset of the lesions seen on a bone scan, confirming the observation made in another study (*13*).

One feature of the antibody 7E11-C5.3 is its binding to a nonshed membrane-bound antigen (*12*) that makes RIS independent of PSA levels, which is important in view of the incidence of prostate cancer with normal or near normal PSA levels (*23*). In the present series, the correlation between RIS and PSA was 12/13 (92%) for clinically localized disease, 7/8 (88%) for incidental disease, and 5/6 (83%) for recurrent disease. In these three categories, there were 3/27 (11%) discordant cases with positive RIS and normal or undetectable PSA levels, with RIS providing the correct information. In known metastatic disease, RIS correlated well with rising PSA levels in 3/3 (100%), but less so in patients with falling PSA levels (3/5, 60%). The overall correlation between PSA levels and RIS was 30/35 (86%) in the present series of patients.

The pattern of "skip" metastases seen with ^{111}In CYT356 (*13*) was not seen in the planar views in this series with no abdominal, thoracic or supraclavicular focal abnormalities. This may be due to the fact that our imaging protocol concentrated on pelvic pathology, with SPECT directed towards this area only due to logistical constraints. With the addition of a new

dual-headed gamma camera to our department, we aim to extend SPECT imaging to include regions other than the pelvis for future patients.

CONCLUSION

These findings suggest that RIS using ^{99m}Tc CYT-351 may have a useful place in staging prostate cancer and monitoring its response to treatment. With further refinement in the data analysis technique, it may be capable of defining the extent of the primary tumor and prove to be a useful adjunct in the staging of primary malignancy when evaluating patients for radical treatment. This ability to image prostatic malignancy in soft tissues and lymph nodes provides a new and clinically useful method for evaluating prostate cancer in the patient with rising PSA levels and a negative bone scan and other negative imaging test results.

ACKNOWLEDGMENTS

We thank Cytogen Corporation, Imperial Cancer Research Fund and St. Bartholomew's Research Trust, and the assistance of all the technical staff, especially Ms. A. Harte and Mrs. J. Suresh in performing the scans.

REFERENCES

1. Scardino PT. Problem of prostate cancer. *J Urol* 1994;152:1677–1678.
2. Gervasi LA, Mata J, Easley JD, et al. Prognostic significance of lymph nodal metastases in prostate cancer. *J Urol* 1989;142:332–336.
3. Paulson DF. Impact of radical prostatectomy in the management of clinically localised disease. *J Urol* 1994;152:1826–1830.
4. Golimbu M, Morales P, Al-Askari, et al. CAT scanning in staging of prostate cancer. *Urology* 1981;3:305–308.
5. Weinerman PM, Arger PH, Pollack HM. CT evaluation of bladder and prostate neoplasms. *Urol Radiol* 1982;4:105–114.
6. Bezzi M, Kressel HY, Allen KS, et al. Prostatic carcinoma: staging with MR imaging at 1.5T. *Radiology* 1988;169:339–346.
7. Hricak H. Noninvasive imaging for staging of prostate cancer: magnetic resonance imaging, computed tomography and ultrasound. *NCI Monogr* 1988;7:31–35.
8. Chisholm GD, Short MD, Ghanadian R, et al. Radiozinc uptake and scintiscanning in prostatic disease. *J Nucl Med* 1974;15:739–742.
9. Bergen B, Coffey DS, Scott WW. Concepts and limitations of radiolabelled antiandrogens, oestrogens, or androgens as isotopic scanning agents for the prostate. *Investig Urol* 1975;13:10–16.
10. Babaian RJ, Lamki LM. Radioimmunoscintigraphy of prostate cancer. *Semin Nucl Med* 1989;4:309–321.
11. Horoszewicz JS, Kawinski E, Murphy GP. Monoclonal antibodies to a new antigenic marker in epithelial prostatic cells and serum of prostatic cancer patients. *Anticancer Res* 1987;7:927–936.
12. Murphy GP. Lucy Wortham James basic research award: markers of prostatic carcinoma. *Arch Surg* 1991;126:1404–1407.
13. Gulfo JV. Clinical utility of monoclonal antibodies in prostate cancer. In: Dawson NA, Vogelzang NJ, eds. *Prostate cancer*. New York: Wiley–Liss;1994:77–94.
14. Mather SJ, Ellison D. Reduction mediated technetium-99m-labeling of monoclonal antibodies. *J Nucl Med* 1990;5:692–697.
15. Stalteri M, Mather SJ, Chengazi VU, et al. Site-specific conjugation and labelling of prostate antibody 7E11C5 with ^{99m}Tc [Abstract]. *Nucl Med Commun* 1995;16:241.
16. Buraggi GL, Turrin A, Cascinelli N, et al. Immunoscintigraphy with antimelanoma monoclonal antibodies. In: Cox P, ed. *Monographs in nuclear medicine, volume 1*. Reading, U.K.: Gordon and Breach Science Publishers;1984:215–253.
17. Britton KE, Granowska M. Radioimmunoscintigraphy in tumor identification. *Cancer Surv* 1987;6:247–267.
18. Babaian RJ, Sayer J, Podoloff DA, et al. Radioimmunoscintigraphy of pelvic lymph nodes with ^{111}In-labeled monoclonal antibody CYT-356. *J Urol* 1994;152:1952–1955.
19. Sanford E, Grzonka R, Heal A, et al. Prostate cancer imaging with a new monoclonal antibody: a preliminary report. *Ann Surg Oncol* 1994;5:400–404.
20. Kotz D. Monoclonal antibody scan holds promise for prostate cancer imaging. *J Nucl Med* 4:1996;11N–15N.
21. O'Connor MK, Kelly BJ. Evaluation of techniques for the elimination of "hot" bladder artefacts in SPECT of the pelvis. *J Nucl Med* 1990;11:1872–1875.
22. Chengazi VU, Nimmon CC, Britton KE. Forward projection analysis and image surgery: an approach to quantitative tomography. International Atomic Energy Agency and World Health Organization Symposium "Tomography in Nuclear Medicine, Present Status and Future Prospects. 1996:31–44.
23. Mettlin C, Murphy GP, Lee F, et al. Characteristics of prostate cancer detected in the American Cancer Society–National Prostate Cancer Detection Project. *J Urol* 1994;152:1737–1740.

Comparison of Technetium-99m-MIBI and Technetium-99m-Tetrofosmin Uptake by Musculoskeletal Sarcomas

Veli Söderlund, Cathrine Jonsson, Henrik C.F. Bauer, Otte Brosjö and Hans Jacobsson

Departments of Diagnostic Radiology, Hospital Physics and Orthopedic Surgery, Karolinska Hospital, Stockholm, Sweden

Technetium-99m-MIBI was initially developed for heart studies but it can also be used to depict tumors, predict multidrug resistance and evaluate chemotherapy. Recently, ^{99m}Tc-tetrofosmin, which exhibits similar physical properties, has been launched for heart studies. Tumor uptake and prediction of multidrug resistance have also been reported regarding the latter tracer. A comparison of these two tracers regarding the detectability of musculoskeletal sarcoma has been made. **Methods:** Twenty patients with musculoskeletal sarcoma of the extremities or pelvis underwent planar examination after the administration of ^{99m}Tc-MIBI and ^{99m}Tc-tetrofosmin with an interval of 2–7 days. The tumor activity was compared with one ipsilateral and one contralateral background region. **Results:** There was a small, but not significant, difference in favor of ^{99m}Tc-MIBI with regard to both background regions. **Conclusion:** Technetium-99m-MIBI and ^{99m}Tc-tetrofosmin can both be used to visualize musculoskeletal sarcomas. The choice may depend on which agent is used routinely for myocardial studies in the laboratory.

Key Words: musculoskeletal sarcoma; technetium-99m-MIBI; technetium-99m-tetrofosmin; tumor imaging

Received Jun. 5, 1996; accepted Oct. 2, 1996.

For correspondence or reprints contact: Hans Jacobsson, MD, Dept. of Diagnostic Radiology, Karolinska Hospital, S-171 76 Stockholm, Sweden.

J Nucl Med 1997; 38:682–686

Various radiopharmaceuticals have been explored for use in tumor detection and characterization. Technetium-99m-hexakis-2-methoxyisobutyl isonitrile (^{99m}Tc-MIBI, ^{99m}Tc-sestamibi, RP-30, Cardiolite®) was developed for myocardial studies (*1,2*). After the incidental detection of a lung metastasis at cardiac imaging (*3*), several case reports describing tracer uptake in various tumors appeared (*4–8*) and several articles reporting uptake in series of tumors have recently been published (*9–13*). In addition, it has been suggested that ^{99m}Tc-MIBI may be used for the prediction of multidrug resistance (MDR) as well as for response evaluation after chemotherapy (*14,15*). Consequently, ^{99m}Tc-MIBI must be considered to be an established agent for nuclear oncology as well.

Recently, ^{99m}Tc-1,2-bis[bis(2-ethoxyethyl)phosphino]ethane (^{99m}Tc-tetrofosmin, P53, PPN0.1011, Myoview®) has been launched for myocardial studies (*16,17*). The functional characteristics of this agent are similar to those of ^{99m}Tc-MIBI. Uptake in malignant lesions have been described, and a potential as a predictor of MDR in breast cancer has been suggested (*18–22*).